THE ASTROPHYSICAL JOURNAL, 506:L35–L38, 1998 October 10

THE X-RAY SPECTRUM OF SAX J1808.4−3658

W. A. HEINDL[1] AND D. M. SMITH[2]

Received 1998 May 28; accepted 1998 August 5; published 1998 September 9

ABSTRACT

We report on the X-ray spectrum of the 401 Hz X-ray pulsar and type I burst source SAX J1808.4−3658 during its 1998 April/May hard outburst. The observations were made with the *Rossi X-ray Timing Explorer* (*RXTE*) over a period of 3 weeks. The spectrum is well described by a power law with a photon index of 1.86 ± 0.01 that is exponentially cutoff at high energies. Excess soft emission above the power law is present as well as a weak Fe-K line. This is the first truly simultaneous broadband (2.5–250 keV) spectrum of a type I burst source in the hard state. The spectrum is consistent with other hard-state burster spectra that cover either only the soft (1–20 keV) or hard ($\gtrsim$20 keV) bands or cover both, but not simultaneously. The cutoff power-law spectrum resembles that of black hole candidates in their low states observed with *RXTE*. We compare the SAX J1808.4−3658 spectrum to three black hole candidates and find that the power law is somewhat softer. This suggests that the photon index may provide a way to distinguish between low-state emission from Galactic black holes and type I bursters.

Subject headings: stars: individual (SAX J1808.4−3658) — stars: neutron — X-rays: stars

1. INTRODUCTION

SAX J1808.4−3658 is the first object thought to display both type I X-ray bursts and coherent X-ray pulsations. Its low implied magnetic field ($B \lesssim 2 \times 10^8$ G; Wijnands & van der Klis 1998b) and high spin frequency may make SAX J1808.4−3658 a missing link in the evolution of the millisecond radio pulsars. It was discovered in observations of the Galactic center region made during 1996 September 12–17 with the Wide Field Camera on *BeppoSAX* (in't Zand et al. 1998). During 6 days of observations, the flux level was ~50–100 mCrab (2–10 keV). Earlier and later observations that did not detect the source limit the outburst duration to between 6 and 40 days. This duration was confirmed with data from the All Sky Monitor (ASM) on the *Rossi X-Ray Timing Explorer* (*RXTE*), which detected SAX J1808.4−3658 for about 20 days beginning 1996 September 8 (in't Zand et al. 1998). Two type I X-ray bursts were also detected during the *BeppoSAX* observations, making the identification of the source as a neutron star in a low-mass X-ray binary highly probable. Assuming that these bursts reached the Eddington luminosity for a 1.4 $M_\odot$ neutron star implies a distance of ~4 kpc.

Following the 1996 outburst, SAX J1808.4−3658 remained undetected until a slew of the *RXTE* pointed instruments on 1998 April 9 serendipitously detected a source (designated XTE J1808−3658) whose location is consistent with the *BeppoSAX* error region (Marshall 1998). The flux level at this time was ~50 mCrab (2–10 keV), corresponding to a luminosity of 1.5×10^{36} ergs s^{-1} at a distance of 4 kpc. Twenty-one *RXTE* pointed observations over the next 4 weeks saw the flux increase to 60 mCrab (2.5–20 keV) and decrease approximately exponentially with a time constant of about 10 days (see Fig. 1). After May 26, the source dimmed rapidly by a factor of ~5 in 2 days.

Timing analyses of *RXTE*/Proportional Counter Array (PCA) data from 1998 April 11 revealed that SAX J1808.4−3658 is an X-ray pulsar with a frequency of 401 Hz, making it the first accretion-powered millisecond X-ray pulsar (Wijnands & van der Klis 1998a, 1998b). The pulsed amplitude was quite low, only ~4% rms (2–60 keV). Chakrabarty & Morgan (1998a), also using PCA data, detected the binary orbit. They derived an orbital period of 7249.119(1) s, a projected semimajor axis of $a_x \sin i = 62.809(1)$ lt-ms, and an X-ray mass function of 3.85×10^{-5} $M_\odot$ (Chakrabarty & Morgan 1998b). They also placed upper limits on the pulse frequency derivative and the eccentricity (less than 5×10^{-4}) of the orbit. The very small mass function implies that the companion mass is less than 0.18 $M_\odot$ for a neutron star less massive than 2 $M_\odot$ (Chakrabarty & Morgan 1998b).

During the recent X-ray outburst, optical imaging of the SAX J1808.4−3658 field revealed an object with magnitude $V = 16.6$ that was not present in the Digitized Sky Survey to a limiting magnitude of $V > 19$ (Roche et al. 1998). This object was confirmed as the likely optical counterpart of SAX J1808.4−3658 when multiple *V*-band exposures covering the 2 hr binary orbit showed "roughly sinusoidal" variability of 0.12 mag (Giles, Hill, & Greenhill 1998).

Early work with the *RXTE* data indicated that the SAX J1808.4−3658 spectrum was Crab-like and continued unbroken to energies greater than 100 keV (Heindl, Marsden, & Blanco 1998; Giles et al. 1998). In this Letter, we perform detailed spectral studies and show that the spectrum is somewhat harder than the Crab at low energies ($\lesssim$30 keV) and is exponentially cutoff at higher energies.

2. OBSERVATIONS AND ANALYSIS

The recent outburst was the subject of a monitoring campaign with the PCA and the High Energy X-ray Timing Experiment (HEXTE) on *RXTE*. The PCA (Jahoda et al. 1996) is a set of five xenon proportional counters (2–60 keV) with a total area of ~7000 cm^2. The HEXTE consists of two clusters of four NaI(Tl)/CsI(Na) phoswich scintillation counters (15–250 keV) totaling ~1600 cm^2 area (Gruber et al. 1996; Rothschild et al. 1998). The two clusters alternate rocking between source and background fields to measure the background. The PCA and HEXTE share a common 1° FWHM field of view. In this Letter, we discuss the X-ray spectra obtained during 13 observations made between 1998 April 11 and 25. Figure 1 shows the flux

[1] Center for Astrophysics and Space Sciences, Code 0424, University of California, San Diego, La Jolla, CA 92093; wheindl@ucsd.edu.
[2] Space Sciences Laboratory, University of California, Berkeley, Berkeley, CA 94720.

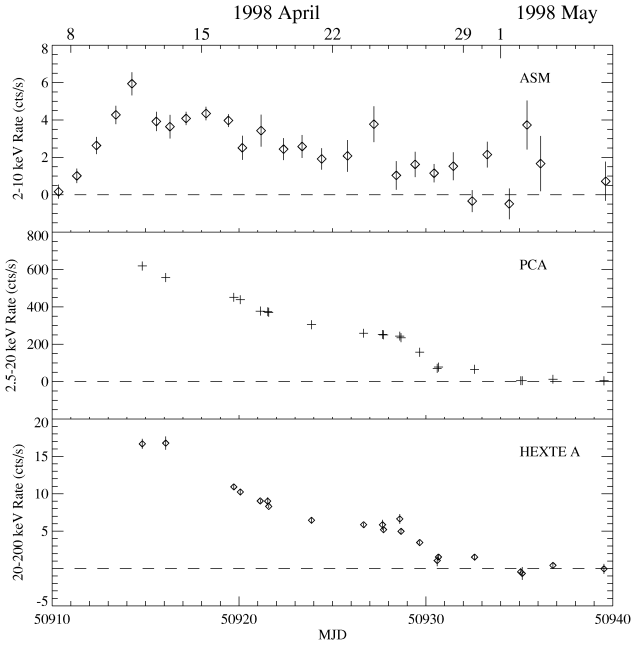

FIG. 1.—Light curve of the 1998 April outburst of SAX J1808.4−3658 in three energy bands from the ASM, PCA, and HEXTE on *RXTE*.

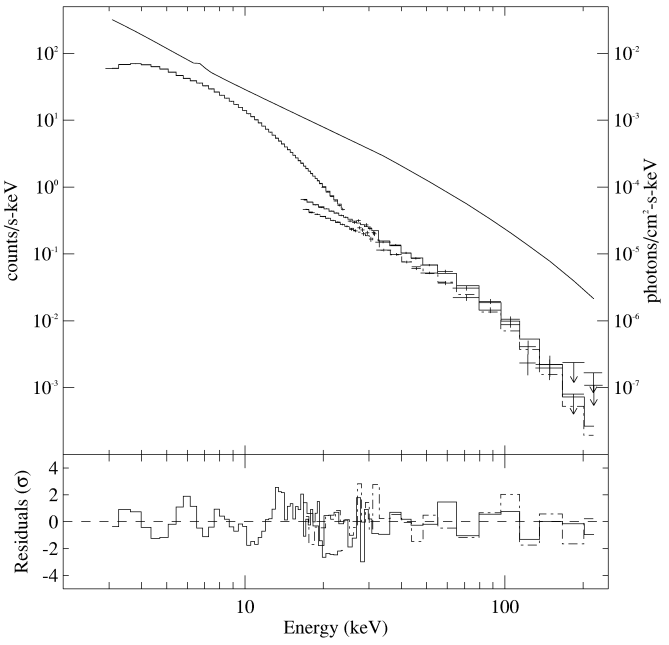

FIG. 2.—Spectrum of SAX J1808.4−3658 between MJD 50914 and 50928. The upper panel shows the measured and best-fit counts spectra (*data points* and *histograms*) and the inferred incident photon spectrum (*smooth curve*).

history of SAX J1808.4−3658 in three energy bands. The ASM data are the publicly available daily averages provided by the ASM/*RXTE* team.[3] The outburst peaked between April 10 and 12 and declined over the next 20 days.

For each observation, we accumulated PCA and HEXTE spectra without regard to the binary orbit and the X-ray pulse phase. These spectra are quite hard, being superficially similar to the Crab Nebula and pulsar (a power law with photon index of ∼2) and extending to over 100 keV (Heindl et al. 1998; Gilfanov et al. 1998). The PCA background was estimated using PCABACKEST version 1.5, with the background model based on blank-sky pointings. We then used XSPEC to fit various models to the observed counts spectra. PCABACKEST and XSPEC are standard NASA software tools. In all fits, the relative normalizations of the PCA and the two HEXTE clusters were taken as free parameters owing to uncertainties ($\lesssim$5%) in the HEXTE dead time measurement. We then verified that the fitted relative normalizations were consistent with those derived from fits to the Crab.

No single-component model could adequately fit the full 2.5–250 keV spectrum. In particular, excess emission above a power law at low energies ($\lesssim$10 keV), Fe-K line emission, and (for the more significant observations) a cutoff at high energies ($\gtrsim$35 keV) are all required. Several complex models fit the spectra with acceptable χ^2. For example, the broadband continuum (above the Fe-K line) could be fit by any of a broken power law, a power law with an exponential cutoff above ∼30 keV, or a Comptonized spectrum (Sunyaev & Titarchuk 1980). Further, a black body, a disk (multicolor) black body (see, e.g., Mitsuda et al. 1984; Makishima et al. 1986), and a thermal bremsstrahlung model were all adequate to reproduce the low-energy excess.

Because it provided the best fits and is simple in form, we concentrated on a model made up of a power law with an exponential cutoff at high energies ($E^{-\Gamma}$, $E \le E_{\rm cut}$; $E^{-\Gamma} \times e^{-(E-E_{\rm cut})/E_{\rm fold}}$, $E > E_{\rm cut}$) plus a Gaussian Fe-K line and a disk black body. Low-energy absorption due to intervening interstellar and/or local gas was also allowed.

Fits to the individual pointings showed no evidence for spectral variability prior to the rapid dimming of the source, which began around MJD 50929. Spectra after this time may have been slightly softer, but the change was not highly significant. We therefore added all of the data prior to that date to obtain the most significant spectrum. The PCA data below 25 keV are of extremely high statistical significance, so that uncertainties are dominated by small systematics in the instrument response matrix. We applied systematic errors to the spectrum of between 0.5% and 2% of the count rate per channel, inferred from fits to the Crab. In addition, we fixed the Gaussian width of the Fe-K line at 0.1 keV (σ), which is narrow compared to the PCA energy resolution.

3. RESULTS

The total spectrum for observations between MJD 50914 and 50928 together with the best-fit model and the inferred incident spectrum of the form described above are shown in Figure 2. The model parameters are listed in Table 1. Although we included systematic uncertainties in the PCA data, we were concerned that the residuals to a simple power-law model may have been caused by small errors in the response matrix. So, to verify our results, we divided the PCA data by a Crab Nebula and pulsar spectrum (provided by K. Jahoda of the PCA team) that was obtained on MJD 50914. The ratio is shown in Figure 3. Because the Crab is a very bright source, the statistics of its spectrum are negligible in the ratio. Since the spectrum of SAX J1808.4−3658 is similar in overall shape, the ratio gives a fairly matrix-independent picture of features that differ from the Crab. In particular, the overall positive slope is due to the harder power law in SAX J1808.4−3658, and the soft excess and an iron line are clear below 10 keV. While we remain

[3] These daily averages are available at http://heasarc.gsfc.nasa.gov/docs/xte/asm_products.html.

TABLE 1

SPECTRAL FITS TO THE X-RAY BURSTER SAX J1808.4−3658 AND THREE BLACK HOLE CANDIDATES

Parameter	SAX J1808.4−3658	Cyg X-1	1E 1740.7−2942	GRS 1758−258
$N_{\rm H}$ ($\times$ 10^{22} cm^{-2})	$0.37^{+0.26}_{-0.21}$	0.3 ± 0.2	8.6 ± 0.6	1.3 ± 0.3
$T_{\rm in}$[a] (keV)	$0.99^{+0.08}_{-0.02}$	1.4 ± 0.1	1.15 ± 0.30	1.4 ± 0.2
$K_{\rm dbb}$[b]	13^{+2}_{-5}	18 ± 4	$1.2^{+0.8}_{-0.5}$	$0.87^{+.99}_{-.30}$
$E_{\rm Fe}$ (keV)	$6.8^{+0.1}_{-0.2}$	$6.47^{+0.06}_{-0.09}$	5.7 ± 0.7[c]	$6.28^{+0.12}_{-0.07}$[c]
$\rm EW_{Fe}$ (eV)[d]	52^{+9}_{-8}	90^{+13}_{-8}	19^{+19}_{-14}[c]	77 ± 9[c]
Γ[e]	1.86 ± 0.01	1.488 ± 0.014	1.53 ± 0.06	1.54 ± 0.04
$E_{\rm cut}$ (keV)	34 ± 4	34 ± 5	19.1 ± 3.5	30^{+20}_{-10}
$E_{\rm fold}$ (keV)	127^{+22}_{-13}	230 ± 20	116 ± 20	185^{+75}_{-50}
$L_{\rm 1–20keV}$[f]	2.5	5.2	7.0	5.7
$L_{\rm 20–200keV}$[f]	1.9	11	15	12

[a] Temperature at the disk inner edge.

[b] Normalization of the disk blackbody component: $K_{\rm dbb} = (R_{\rm in}/D_{10})\cos\theta$. $R_{\rm in}$ is the disk inner radius in kilometers, D_{10} is the distance in units of 10 kpc, and θ is the angle of the disk.

[c] Additional systematic uncertainties apply due to the subtraction of diffuse Galactic plane Fe-K emission.

[d] Fe-K line equivalent width.

[e] Power-law photon index.

[f] Luminosity (10^{36} ergs s^{-1}). Assuming distances of 4 kpc to SAX J1808.4−3658, 1.9 kpc to Cyg X-1, 8.5 kpc to 1E 1740.7−2942, and 8.5 kpc to GRS 1758−258.

cautious of the physical interpretation of the soft excess as a disk black body and the quantitative iron line model parameters, we are confident that both the soft excess and the iron line are present.

Figure 3 also shows that the resemblance to the Crab is at best superficial. In contrast to the power-law fits to the individual observations made by Gilfanov et al. (1998), we find strong deviations from such a simple model ($\chi^2_{\rm red} = 22.4$ with 94 degrees of freedom [dof]), even in the limited range of 3–100 keV that they used. The most important excursions are at low and high energies, where we find a soft excess and an exponential cutoff, respectively. The fit in Table 1 for SAX J1808.4−3658 had $\chi^2_{\rm red} = 1.65$ for 99 dof (2.5–250 keV). If we disallow the exponential cutoff and refit all of the other parameters, we find $\chi^2_{\rm red} = 4.34$ for 101 dof. Applying an *F*-test (Bevington 1969) to the ratio of the improvement in χ^2 and χ^2 of the full model (divided by 2 and 99 dof, respectively), we find that the probability that the cutoff is unnecessary is only 7×10^{-22}.

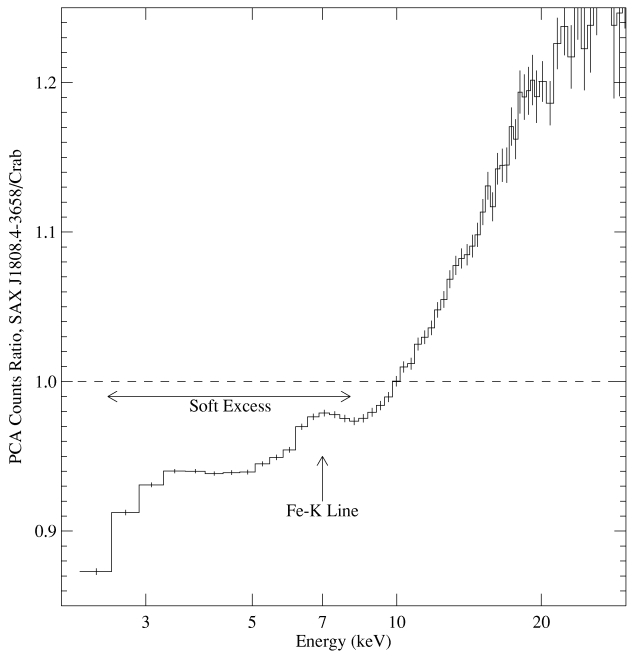

FIG. 3.—Ratio of the PCA counts spectra of SAX J1808.4−3658 and the Crab Nebula and pulsar. The data have been arbitrarily normalized to 1 at 10 keV.

We also analyzed the PCA spectra in eight bins by orbital phase. Due to the limited amount of data, each phase bin samples the different parts of the decaying light curve to different degrees. To compensate for this effect, we fit an exponential decay to the light curve and looked for additional variations. We find an apparent intensity variation with orbit, in agreement with Chakrabarty & Morgan (1998b): roughly sinusoidal, with an amplitude of 2% and a minimum when the neutron star is behind its companion. The modulation is several times larger than could be explained by uncertainties in the background model. We find no differences in the spectrum with phase: the disk black body and power-law components share the extinction equally, and the absorption column is unchanged. This may imply that the modulation is due to Compton scattering in a thin, ionized intervening medium (e.g., the ablated wind suggested by Chakrabarty & Morgan 1998b), which would scatter photons out of the line of sight nearly independently of energy. Alternately, the modulation could be an artifact of the limited amount of data, caused by random correlations between the orbital phase and small variations in the accretion rate: the total amount of data available is only about 14 orbits.

4. DISCUSSION

4.1. *Comparison to Type I Burst Sources*

Prior to this work, the only bursters with nearly simultaneous coverage of the X-ray and hard X-ray bands during episodes of hard outburst were Cen X-4 and 4U 1608−52. In 1979, Cen X-4 was observed with *Hakucho* (1.5–30 keV; Matsuoka et al. 1980), *Ariel 5* (3–6 keV; Kaluzienski, Holt, & Swank 1980), and *Prognoz 7* (13–163 keV; Bouchacourt et al. 1984). Bouchacourt et al. (1984) fit the *Prognoz 7* spectrum to a hard power law (photon index fixed: $\Gamma \equiv 1$) times an exponential cutoff with a folding energy of ~50 keV—not unlike the *RXTE* SAX J1808.4−3658 spectrum. They also noted that the low-energy extrapolation of the *Prognoz 7* data fell below the simultaneous *Ariel 5* spectrum, suggesting soft excess emission, although this could be due to the true photon index differing from 1. Zhang et al. (1996) used the *Ginga* spectrum (Yoshida et al. 1993) from the middle of a ~170 day (1991

June–December) outburst to constrain the low-energy portion of the 4U 1608−52 spectrum observed by BATSE. The *Ginga* data showed a power law with a photon index of -1.75 ± 0.01, and together with the BATSE data the spectrum was fit by a Comptonized model (Sunyaev & Titarchuk 1980) with $kT = 23$ keV and optical depth 4.4 (for a spherical geometry). For SAX J1808.4−3658, we find nearly identical values of $22.0^{+1.6}_{-0.8}$ keV and $4.02^{+0.11}_{-0.15}$ for the electron temperature and optical depth. Thus, the broadband spectra of all three well-studied hard-state burst sources are quite similar.

Hard X-ray emission from other bursters has been observed (without concurrent soft X-ray coverage) with BATSE and SIGMA (see Barret, McClintock, & Grindlay 1996 and references therein). When these data are fit to broken power-law spectra, photon indices of between 2.5 and 3 above the break are generally found. Fitting the HEXTE data above 40 keV gives an index of 2.4 ± 0.1 for SAX J1808.4−3658, in reasonable agreement with the high-energy spectra of other low-state bursters.

4.2. *Comparison to Black Hole Candidates*

Historically, hard emission extending to $\gtrsim$100 keV from X-ray binaries has been considered a "black hole signature," distinguishing black hole sources from low magnetic field neutron stars. Clearly with several burst sources emitting hard X-rays, the situation is not so simple. However, it may still be possible to separate these neutron stars by other properties of their emission. For example, Barret et al. (1996) noted that neutron stars only produce hard tails when the tails dominate the emission, as opposed to black holes, which can produce hard tails along with very bright ultrasoft emission. They also noted that the luminosity when the hard emission dominates can be higher for black holes than for neutron stars. SAX J1808.4−3658 is consistent with a neutron star by both of these criteria, showing only a very weak soft component and having a modest luminosity ($\sim 5 \times 10^{36}$ ergs s^{-1} assuming a distance of 4 kpc). Given that distances are often poorly known and that black hole candidates can also be seen at low luminosities, luminosity alone is an insufficient means to distinguish between source types.

To see if the spectrum alone can serve the purpose, we fit *RXTE* observations of the persistent low-state black hole candidates (BHCs) Cyg X-1 (1998 April), 1E 1740.7−2942 (1996 March), and GRS 1758−258 (1996 August) to the same model used for SAX J1808.4−3658. These fits are listed in Table 1. One feature of the BHC spectra clearly differs from the bursters: the photon indices are significantly harder in the BHCs. The BHCs' power laws are between 1.4 and 1.6, while the SAX J1808.4−3658 index is 1.86. From *Ginga* observations, 4U 1608−522 had an index of 1.75 during the period of hard emission described above. Thus, from this limited sample, the broadband spectrum separates the BHCs and neutron stars via the hardness of the power law. Given the realities of intercalibrating multiple instruments and the modest separation of the indices, this characteristic may be difficult to use for comparisons between different observatories. However, it will clearly be useful for observations made with a single instrument complement or between instruments that are well intercalibrated.

5. CONCLUSIONS

The spectrum of the unique 401 Hz pulsar and type I burster SAX J1808.4−3658 during its recent outburst was quite hard. The photon spectral index was 1.86, with a slow cutoff at high energies. There was clear evidence of excess soft emission and a weak Fe-K line. These *RXTE* observations have provided the highest quality broadband spectrum of a suspected X-ray burster during a period of hard emission. The spectrum is in good agreement with previous observations of other bursters made over more limited energy bands and with lower statistical significance. By comparing to observations of low-state BHCs, we find that BHCs and bursters can be distinguished by the slope of their power-law emission. In particular, the photon indices of bursters are greater (i.e., softer) by about 0.3, even though the overall spectral shapes are quite similar.

Thanks to Keith Jahoda for his help with the PCA response matrix and for providing the Crab data. We would also like to acknowledge the *RXTE* Science Operations Center for scheduling these Target of Opportunity observations. This work was supported by NASA grant NAS5-30720.

REFERENCES

Barret, D., McClintock, J. E., & Grindlay, J. E. 1996, ApJ, 473, 963
Bevington, P. R. 1969, Data Reduction and Error Analysis for the Physical Sciences (New York: McGraw-Hill), 200
Bouchacourt, P., Chambon, G., Niel, M., Refloch, A., Estulin, I. V., Kuznetsov, A. V., & Melioranskii, A. S. 1984, ApJ, 285, L67
Chakrabarty, D., & Morgan, E. H. 1998a, IAU Circ. 6877
———. 1998b, Nature, 394, 346
Giles, A. B., Hill, K. M., & Greenhill, J. G. 1998, IAU Circ. 6886
Gilfanov, M., et al. 1998, preprint (astro-ph/9805152)
Gruber, D. E., Blanco, P. R., Heindl, W. A., Pelling, M. R., Rothschild, R. E., & Hink, P. L. 1996, A&AS, 120, 641
Heindl, W. A., Marsden, D., & Blanco, P. 1998, IAU Circ. 6878
in't Zand, J. J. M., Heise, J., Muller, J. M., Bazzano, A., Cocchi, M., Natallucci, L., & Ubertini, P. 1998, A&A, 331, L25
Jahoda, K., Swank, J. H., Giles, A. B., Stark, M. J., Strohmayer, T., Zhang, W., & Morgan, E. H. 1996, Proc. SPIE, 2808, 59
Kaluzienski, L. J., Holt, S. S., & Swank, J. H. 1980, ApJ, 241, 779
Makishima, K., Maijima, Y., Mitsuda, K., Bradt, H. V., Remillard, R. A., Tuohy, I. R., Hoshi, R., & Nakagawa, M. 1984, ApJ, 308, 635
Marshall, F. E. 1998, IAU Circ. 6876
Matsuoka, M., et al. 1980, ApJ, 240, L137
Mitsuda, K., et al. 1984, PASJ, 36, 741
Roche, P., Chakrabarty, D., Morales-Rueda, L., Hynes, R., Slivan, S. M., Simpson, C., & Hewett, P. 1998, IAU Circ. 6885
Rothschild, R. E., et al. 1998, ApJ, 496, 538
Sunyaev, R. A., & Titarchuk, L. G. 1980, A&A, 86, 121
Wijnands, R., & van der Klis, M. 1998a, IAU Circ. 6876
———. 1998b, Nature, 394, 344
Yoshida, K., Mitsuda, K., Ebisawa, K., Ueda, Y., Fujimoto, R., Yaqoob, T., & Done, C. 1993, PASJ, 45, 605
Zhang, S. N., et al. 1996, A&AS, 120, 279